More than a Catharanthus plant: A multicellular and pluri-organelle alkaloid-producing factory

Natalja Kulagina, Louis-Valentin Méteignier, Nicolas Papon, Sarah Ellen O'Connor, Vincent Courdavault

Version of Record: https://www.sciencedirect.com/science/article/pii/S1369526622000292
Manuscript_31fa4cb0ee58849e8a20fdaea86a25a4

REVIEW

More than a Catharanthus plant: a multicellular and pluri-organelle alkaloid-producing factory

Natalja Kulagina[1], Louis-Valentin Méteignier[1], Nicolas Papon[2], Sarah Ellen O'Connor#[3], Vincent Courdavault#[1]

[1] Université de Tours, EA2106 Biomolécules et Biotechnologies Végétales, Tours, France

[2] Univ Angers, Univ Brest, IRF, SFR ICAT, F-49000 Angers, France.

[3] Department of Natural Product Biosynthesis, Max Planck Institute for Chemical Ecology, Jena 07745, Germany.

corresponding author: oconnor@ice.mpg.de ; vincent.courdavault@univ-tours.fr

Graphical abstract

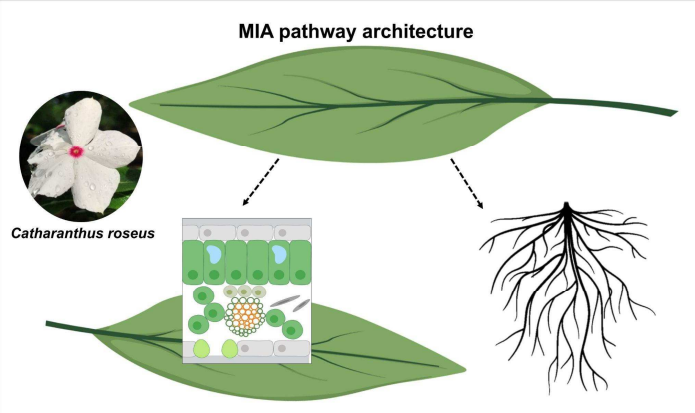

Abstract

Plants represent a huge reservoir of natural products. A broad series of these compounds now find application for human health. In this respect, the monoterpene indole alkaloids (MIAs), particularly from Madagascar periwinkle, are a prominent example of plant specialized metabolites with an important therapeutic potential. However, the supply of MIA drugs has always been a challenge since the low-yield accumulation *in planta*. This mainly results from the complex architecture of the MIA biosynthetic pathway that involves several organs, tissue types and subcellular organelles. Here, we describe the most recent advances towards the elucidation of this pathway route as well as its spatial organization *in planta*. Besides allowing a better understanding of the MIA biosynthetic flux in the whole plant, such knowledge will also probably pave the way for the development of metabolic engineering strategies to sustain the MIA supply.

Highlights

- **Plant specialized metabolism contributes to their adaptation and defenses.**
- ***Catharanthus roseus* produces in low quantities therapeutic monoterpene indole alkaloids (MIAs), including the most active anticancer drugs.**
- **To date, several missing enzymes downstream strictosidine have been identified, as well as specific transporters.**
- ***C. roseus* spatial architecture involves at least three tissue types and eight organelles.**
- **Heterologous production offers an alternative approach, which requires an exhaustive view and characterization of MIA metabolic fluxes.**

Keywords: *Cathranthus roseus*, plant specialized metabolism**,** monoterpene indole alkaloids, transport, localization

Introduction

Plant metabolism can be divided into two main classes: a core (primary) metabolism used to generate energy to enable growth and development, and a specialized metabolism (previously known as secondary metabolism) that builds further sophisticated biomolecules for environmental adaptation and plant speciation. Apart from their *in planta* functions, specialized metabolites are also highly valuable for human health, acting for instance as anticancer drugs or painkillers [1].

While usually distinctly considered, these two types of metabolism are intimately interconnected [2]. Specialized metabolites such as triterpenes and monoterpene indole alkaloids (MIAs) are structurally diverse and respectively rich in C and N atoms, and therefore rely on a supply of carbohydrates and amino acids. More strikingly, a recent groundbreaking study demonstrated that β-NAD, a core metabolite involved in a myriad of biological processes, is a scaffold molecule for specialized metabolites in bacteria [3]. For plants that evolved more diverse and complex metabolic pathways, modeling and system-level approaches have provided insights into the deep intertwining of core and specialized metabolism at the transcriptional and metabolic levels [4]. For instance, the synthesis of glucosinolates specialized metabolites relies on the core tricarboxylic acid pathway and is controlled by shared transcription factors [5]. In addition, while specialized metabolisms have evolved from core metabolism [6,7], there is an increasing body of evidence suggesting that specialized metabolites influence primary metabolism and *vice versa* [8].

MIAs form a prominent class of specialized metabolites of interest [9] and result from the condensation of terpene and indole core building blocks. While the secologanin terpene moiety is synthesized by the plastidial methylerythritol-phosphate pathway, the tryptamine indole moiety emanates from aromatic amino acids produced by the shikimate core pathway, thus highlighting a direct connection with primary metabolism. Historically, most of the research effort dedicated to MIAs has been focused on the Madagascar periwinkle, *Catharanthus roseus*, a medicinal plant that accumulates the anticancer MIAs vinblastine and vincristine. The synthesis of both compounds results from a long and complex biosynthetic pathway, involving the formation of the MIA universal precursor strictosidine via secologanin and tryptamine condensation, and ending with the dimerization of the two precursors vindoline and catharanthine in *C. roseus* leaves. Over years, this pathway has progressively reached the status of a model for plant specialized metabolisms, both in terms of complexity and spatial organization at both the cellular and subcellular levels [10]. Recently, the MIA biosynthetic route towards vincristine and vinblastine reached a near completion allowing to deepen our knowledge of MIA synthesis, and develop yeast factories that produce important MIA precursors, such as strictosidine [11] and vindoline [12,13]. Here, we describe the most recent advances towards the *C. roseus* MIA pathway elucidation with a particular focus on its spatial architecture, probably one of the most complex organizations that plants evolved regarding specialized metabolisms. More specifically, we will focus on the biosynthetic steps following strictosidine formation that were the subject of most recent discoveries.

The MIA pathway architecture around strictosidine

The MIA pathway is highly structured in space and time within *C. roseus* organs, tissues, and subcellular structures, as well reported in leaves (**Figure 1,2**). As previously reviewed [10], the strictosidine synthase (STR) integrates the iridoid and shikimate pathways that occur mainly in the chloroplasts of internal phloem-associated parenchyma (IPAP) cells and the epidermis, respectively (**Figure 2a,b**). Hence, STR condenses the resulting secologanin and tryptamine in the vacuole of leaf epidermal cells through a Pictet-Spengler reaction to produce strictosidine. Strictosidine is further deglycosylated by the strictosidine β-D-glucosidase (SGD) that is targeted to the nucleus to ensure an efficient enzyme/substrate separation. SGD also self-assembles into high molecular multimers that form tubular structures supposed to help in managing the reactivity of the strictosidine aglycone [14]. The formation of such aglycone marks the onset of pathway divergence within the subsequent MIA synthesis. This divergence mainly originates from the highly reactive nature of the strictosidine

aglycone, which spontaneously reorganizes into the more stable 4,21-dehydrogeissoschizine, cathenamine and epi-cathenamine [14]. These intermediates correspond to the substrates of downstream MIA enzymes required for the synthesis of the heteroyohimbine MIA type, including tetrahydroalstonine and ajmalicine [15] (**Figure 2b**), or to the iboga and aspidosperma MIA types such as catharanthine and vindoline, respectively (**Figure 2b,c**) - the two precursors of vinblastine [16].

The synthesis of heteroyohimbine MIAs involves nuclear metabolons

The formation of heteroyohimbine MIAs originates from the strictosidine aglycone intermediates cathenamine and epi-cathenamine, serving as substrates for several tetrahydroalstonine synthase isoforms (THAS1-4) and a heteroyohimbine synthase (HYS) [15,17] (**Figure 2b).** While THAS1-4 only produce tetrahydroalstonine, HYS synthesizes a mixture of three heteroyohimbines including tetrahydroalstonine, 19-epi-ajmalicine (mayumbine) and ajmalicine. Interestingly, all these enzymes interact with the SGD multimers in the nucleus of epidermal cells. Such interactions are thought to prevent the release of the highly reactive aglycone. They are also supposed to favor its spontaneous conversion into the THAS/HYS substrates through a metabolon formation, i.e. a series of enzymes forming a structural-functional complex. Ultimately, the resulting tetrahydroalstonine and ajmalicine are oxidized into alstonine and serpentine by the alstonine synthase (AS) and serpentine synthase (SS), respectively (**Figure 2b)**. Both enzymes are cytochrome P450 anchored to the endoplasmic reticulum (ER), thus suggesting an active transport or a passive diffusion of their substrates from the nucleus into the cytosol in the close ER environment [15,17].

The synthesis of the vinblastine and vincristine precursors occurs throughout the plant

The synthesis of vindoline and catharanthine, the aspidosperma and iboga precursors of the anticancer vinblastine and vincristine, is far more complex with their common steps distributed both in periwinkle leaf epidermis and roots. In the past years, several missing steps downstream SGD have been elucidated through transcriptomic analysis and virus-induced gene silencing (VIGS) (**Figure 2b,c,d)**. The synthesis of both compounds uses 4,21-dehydrogeissoschizine as a starting molecule. Such a process involves the 4,21-dehydrogeissoschizine capture by the nucleo-cytosolic alcohol dehydrogenase geissoschizine synthase (GS) [18••] before its cyclization into cathenamine and epi-cathenamine. This probably relies on a premature release from the SGD multimers and a competition between THAS/HYS and GS for the access to substrates. However, this competing mechanism remains to be discovered since no interactions between GS and SGD have been reported to date. Interestingly, the dramatic increase of the heteroyohimbine content at the expense of vindoline and catharanthine content in the *C. roseus* GS mutant suggests that the MIA ratio may rely on GS, THAS and HYS gene expression levels at least partially [19]. On the other hand, geissoschizine is subsequently oxidized by the ER-anchored cytochrome P450 geissoschizine oxidase (GO), mimicking the sequence of reaction described for heteroyohimbines [18••]. This oxidation yields an unstable preakuammicine aldehyde type intermediate (usually named preakuammicine) and initiates the formation of *Strychnos* MIAs, which requires two successive reductions catalyzed by a cinnamyl alcohol dehydrogenase-like enzyme Redox 1 and an aldo-keto-type reductase Redox 2, to produce stemmadenine (**Figure 2b**) [20•]. Importantly, while Redox 1 uses the unstable GO reaction product, Redox 2 reduces an unstable Redox 1 intermediate, which in the absence of Redox 2 is spontaneously converted to (16*S*/*R*)-dehydroxymethyl-stemmadenine, thus arguing for a coordinated reaction between these two reductases. Stemmadenine is subsequently acetylated by the stemmadenine-*O*-acetyltransferase (SAT) to form *O*-acetylstemmadenine [20•]. This last compound is then oxidized into precondylocarpine acetate by a berberine bridge enzyme-like named precondylocarpine acetate synthase (PAS) [21•]. Surprisingly, PAS is targeted to the vacuole via putative ER-derived vesicles (**Figure 2b**), thus suggesting that the oxidative reaction may occur

during this transport step. Indeed, precondylocarpine acetate needs to be reduced by a medium-chain alcohol dehydrogenase, named dihydroprecondylocarpine synthase (DPAS), which forms homodimers in the cytosol. Interestingly, GS can catalyze the reduction of precondylocarpine acetate *in vitro*, and some researchers have suggested that dihydroprecondylocarpine synthesis may result from concerted DPAS/GS activities [22•]. Finally, the resulting dihydroprecondylocarpine is desacetoxylated through Diels-Alder cyclizations by hydrolase-like enzymes, namely catharanthine synthase (CS) and tabersonine synthase (TS), to generate catharanthine and tabersonine, respectively [21•]. It has to be noted that two additional hydrolases, named vincadifformine synthase (VS) also convert dihydroprecondylocarpine into vincadifformine, a reduced form of tabersonine, mainly occurring in roots [22•]. Most importantly, while CS and TS are soluble enzymes located to the nucleocytosol of epidermal cells, both were reported to interact with DPAS [21•] (**Figure 2b**) to form a kind of new metabolon that may guide the MIA biosynthetic flux. In line, the preferred interaction of DPAS with TS may thus favor the synthesis of tabersonine by facilitating substrate exchange between the two final enzymes of the pathway. Finally, while catharanthine constitutes by itself an end-product, tabersonine and vincadifformine can be further metabolized into more complex MIAs following distinct organ-specific biosynthetic pathways.

The conversion of tabersonine into vindoline in folio

In leaves, tabersonine is converted into vindoline via a well-known 7-step biosynthetic route initiated by tabersonine 16-hydroxylase (T16H) and a 16-hydroxytabersonine 16-*O*-methyltransferase (16OMT) in the leaf epidermis [10] (**Figure 2b)**. The resulting 16 methoxytabersonine is then epoxidized by the ER-anchored cytochrome P450 tabersonine 3-oxygenase (T3O) and reduced by the soluble tabersonine 3-reductase (T3R) to yield 16-methoxy-2,3-dihydro-3-hydroxytabersonine [23,24]. The subsequent step of the pathway, catalyzed by the 16-methoxy-2,3-dihydro-3-hydroxytabersonine *N*-methyltransferase (NMT) initiates the translocation of the MIA intermediates from the leaf epidermis through leaf mesophyll [24,25]. So far, at the cellular level, NMT was considered as a thylakoid-associated enzyme while in fact being targeted to peroxisomes through a noncanonical peroxisome targeting signal [26] (**Figure 2b)**. Although not fully explained to date, this peculiar localization probably affects the translocation of the NMT reaction product up to the specialized cells, laticifers and idioblasts, which host the two last steps of the pathway catalyzed by desacetoxyvindoline 4-hydrolase (D4H) and deacetylvindoline 4-*O*-acetyltransferase (DAT) [24,27] (**Figure 2c**).

New insights into the synthesis of the root-specific MIAs

In roots, tabersonine undergoes a different metabolization initiated by the stereoselective C6,C7-epoxidation of tabersonine catalyzed by the ER-anchored tabersonine epoxidase isoform 1 (TEX1) [28] (**Figure 2d**). This reaction yields to the synthesis of lochnericine, a major root MIA that can be further hydroxylated by a second ER-anchored cytochrome P450 named tabersonine 19-hydrolase (T19H) to produce hörhammericine [29]. Whereas T19H can hydroxylate both tabersonine and lochnericine, TEX1 is highly specific of tabersonine thus suggesting that epoxidation necessarily precedes hydroxylation. Albeit not demonstrated to date, it has been postulated that tissue-specific expressions of TEX1 and T19H may orchestrate this synchronized synthesis to avoid competition between both enzymes and favor the formation of hörhammericine. Ultimately, this last compound can be acetylated into 19-acetylhörhammericine by the cytosolic BAHD tabersonine 19-*O*-acetyltransferase (TAT) [30]. Interestingly, while very similar in terms of structure, vincadifformine cannot be hydroxylated by T19H but rather by another enantioselective ER-anchored cytochrome P450 named vincadifformine 19-hydroxylase (V19H) to generate minovincinine [31] (**Figure 2d**). Surprisingly, V19H is phylogenetically closer to T3O rather than T19H suggesting different evolutionary origins between both enzymes. Such a difference may also reflect the diversification of the stereochemistry of the aspidosperma MIAs including (-)- and (+)-skeletons as observed for (-)-

tabersonine (+)-vincadifformine. By contrast, the cytosolic minovincinine 19-*O*-acetyltransferase (MAT) acetylating minovincinine into echotovenine probably derives from local duplication of a BAHD ancestor common to DAT and TAT, given their proximity in the *C. roseus* genome [30,32].

A complex network of MIA transport *in planta*

The sophisticated MIA pathway architecture implies the shuttling of intermediates at multiple levels, including inter-cellular, subcellular and inter-organ transport (**Figure 1,2**). Although MIA metabolite trafficking has been puzzling, several mechanisms have been recently unveiled. At the cellular level, while the secologanin precursor loganic acid has been proposed to travel from IPAP up to epidermis [33], three nitrate/peptide family transporters (NPF 2.4, NPF 2.5, NPF 2.6) have been described to internalize this compound (**Figure 2a,b**) as well as loganin, secologanin, and 7-deoxyloganic acid in *Xenopus laevis* oocytes [34•]. Their expression in both roots and leaves of *C. roseus,* combined with the localization to plasma membranes thus suggests their involvement in the inter-cellular translocation of biosynthetic intermediates, and more specifically in the import of MIA monoterpene precursor into leaf epidermis. In addition, these transporters may also potentially contribute to inter-organ translocations. Indeed, such an inter-organ transport of secologanin from the roots to the leaves was demonstrated by grafting shoots of a low MIA-accumulating *C. roseus* mutant onto the root system of wild-type plants [35].

At the subcellular level, the first ten biosynthetic steps leading to the biosynthesis of geraniol, including notably the enzymes from the methyl-erythritol pathway, occur in the plastid stroma and stromules [36] (**Figure 2a**). Interestingly, the apparent proximity of stromules with ER has been proposed to facilitate geraniol uptake by the downstream ER-anchored cytochrome P450 geraniol 10-hydroxylase (G10H) in IPAP cells of *C. roseus* leaves. Subsequently, once produced in the vacuole, strictosidine is exported to the cytosol to allow its conversion into downstream MIAs. This translocation is mediated by the tonoplast-localized NPF 2.9 transporter [37••] (**Figure 2b**), which probably plays a key role in the control of the biosynthetic flux in the leaf epidermis. Downstream in the pathway, the vacuolar accumulation of vindoline was proposed to rely on a yet not characterized active proton antiport system that probably occurs in laticifers and idioblasts [38]. The translocation of catharanthine remains also elusive. However, CrTPT2, an ATP-binding cassette transporter, has been shown to secrete catharanthine from the epidermis to cuticular waxes (**Figure 2b**) to cope with microbial pathogens and insects [39]. Such physical separation between catharanthine and vindoline probably explains the low amounts of anhydrovinblastine and related MIA dimers in leaves but also the post-folivory dimerization of both compounds occurring in aggressor guts [40]. This attack-induced dimerization is supposed to keep low amounts of the highly toxic dimers to minimize their effects on the whole plant.

Tracking MIA localization by imaging and metabolic labeling

While most of our knowledge on the MIA pathway organization originates from gene product localizations, *in planta* MIA localizations now provide outstanding complementary information. Initial conclusions were based on differential MIA extractions by dipping intact *C. roseus* leaves in chloroform. This resulted in the specific recovery of catharanthine leading to the claim of its exclusive location on the leaf surface, in agreement with CrTPT2 activity [41] (**Figure 3a**). However, this compartmentalization was recently challenged by a comparative MIA extraction procedure [42] and the localization of catharanthine through mass spectrometry imaging. Indeed, while this approach confirmed almost all MIA and biosynthetic intermediate localizations hypothesized so far, catharanthine was localized in idioblasts/laticifers similar to vindoline, in both stems [43] and leaves [44••], (**Figure 3b**). Such colocalization in vacuoles [38] thus suggests that additional mechanisms, different from physical separation, preclude high levels of dimerization in non-challenged plants. Taken altogether, these data suggest the existence of a complex localization for catharanthine. Indeed, although catharanthine can be extruded to cuticular waxes by CrTPT2, its co-occurrence with

vindoline in idioblast/laticifer vacuoles can also explain the low, but detectable anhydrovinblastine dimer in non-challenged leaves. Interestingly, a multicellular distribution has also been described for strictosidine, ajmalicine and serpentine [44••]. The presence of these MIAs in idioblasts thus suggests the existence of an uncharacterized transport mechanism from the epidermis. While the precise nature of the transported MIAs remains to be elucidated, the *in planta* localization of SS would probably allow to determine whether serpentine is transported upon idioblasts or directly synthesized within these specialized cells after ajmaline transport. Finally, metabolic labeling of MIAs with ^{15}N allowed the detection of catharanthine in roots and flowers [45] (**Figure 3c**) with a specific secretion of catharanthine, besides ajmalicine, serpentine, and yohimbine, in the root external environment [46•]. While their secretion mechanism remains uncharacterized since the CrTPT2 transporter is poorly expressed in roots [47], these secreted MIAs probably mediate important communications with microorganisms.

Conclusion and future directions

Thanks to more than four decades of active research, the global architecture of MIAs biosynthetic pathway in *C. roseus* is now fairly deciphered. These investigations have been in particular accelerated recently with the development of different technologies including high-quality genome sequencing, transcriptomic and metabolomic analysis, fluorescence microscopy imaging, and metabolic labeling. All these advancements have not only allowed the identification of missing enzymes but also provided unprecedented insights into the spatial organization of the Madagascar periwinkle MIA pathways at both the cellular and subcellular levels. This teaches us that Catharanthus logistic is likely one of the most complex described to date but beyond this, crucial questions remain to be addressed. For instance, the mechanisms that regulate cell-specific expression of MIA genes are still unknown. Single-cell holistic strategies aiming at identifying *cistrans* (DNA sequence/DNA-binding protein) regulatory modules appear thus critical for answering this question [48]. Besides transcription factors, several other mechanisms have been shown to mediate cell differentiation, like translational and chromatin regulation [49–51]. In the context of MIAs and plant specialized metabolism in general, where genes are in some cases organized into metabolic gene clusters [52,53], the regulation of the 3D conformation of chromatin may have a key role in the expression of MIA gene clusters in specific cell types. In addition, although VIGS has allowed the functional validation of many biosynthetic candidate genes so far, an easily scalable and robust stable transformation method for *C. roseus* is missing for complete gene invalidation using the CRISPR/Cas9 approach for instance. Such a development is of paramount importance for a better understanding of the periwinkle factory.

Beyond understanding MIA biosynthesis *in planta*, elucidating the spatial organization of the pathway also provides new perspectives for MIA metabolic engineering. Indeed, an adapted subcellular localization of biosynthetic enzymes in heterologous expression hosts (e.g. addressed to a non-native organelle) can dramatically increase biosynthetic yields as recently reported for other natural products [54–57]. A better knowledge of these regulatory processes would benefit the rational design of MIA metabolic engineering, as recently reported for vindoline [12,13].

Acknowledgment

We acknowledge funding from the ARD2020 Biopharmaceutical program of the Région Centre Val de Loire (ETOPOCentre project) and ANR MIACYC (ANR-20-CE43-0010).

References

The articles of particular interest published within the last five years are highlighted as:

- of special interest

•• of remarkable interest

1. Debnath B, Singh WS, Das M, Goswami S, Singh MK, Maiti D, Manna K: **Role of plant alkaloids on human health: A review of biological activities**. *Mater Today Chem* 2018, **9**:56–72.

2. Pott DM, Osorio S, Vallarino JG: **From Central to Specialized Metabolism: An Overview of Some Secondary Compounds Derived From the Primary Metabolism for Their Role in Conferring Nutritional and Organoleptic Characteristics to Fruit**. *Front Plant Sci* 2019, **10**:835.

3. Barra L, Awakawa T, Shirai K, Hu Z, Bashiri G, Abe I: **β-NAD as a building block in natural product biosynthesis**. *Nature* 2021, **600**:754–758.

4. Clark TJ, Guo L, Morgan J, Schwender J: **Modeling Plant Metabolism: From Network Reconstruction to Mechanistic Models**. *Annu Rev Plant Biol* 2020, **71**:303–326.

5. Tang M, Li B, Zhou X, Bolt T, Li JJ, Cruz N, Gaudinier A, Ngo R, Clark-Wiest C, Kliebenstein DJ, et al.: **A genome-scale TF-DNA interaction network of transcriptional regulation of Arabidopsis primary and specialized metabolism.** *Mol Syst Biol* 2021, **17**:e10625.

6. Carrington Y, Guo J, Le CH, Fillo A, Kwon J, Tran LT, Ehlting J: **Evolution of a secondary metabolic pathway from primary metabolism: shikimate and quinate biosynthesis in plants.** *Plant J* 2018, doi:10.1111/tpj.13990.

7. Maeda HA: **Evolutionary Diversification of Primary Metabolism and Its Contribution to Plant Chemical Diversity** . *Front Plant Sci* 2019, **10**:881.

8. Erb M, Kliebenstein DJ: **Plant Secondary Metabolites as Defenses, Regulators, and Primary Metabolites: The Blurred Functional Trichotomy.** *Plant Physiol* 2020, **184**:39–52.

9. Kumar S, Singh B, Singh R: **Catharanthus roseus (L.) G. Don: A review of its ethnobotany, phytochemistry, ethnopharmacology and toxicities.** *J Ethnopharmacol* 2022, **284**:114647.

10. Courdavault V, Papon N, Clastre M, Giglioli-Guivarc'h N, St-Pierre B, Burlat V: **A look inside an alkaloid multisite plant: The Catharanthus logistics**. *Curr Opin Plant Biol* 2014, **19**:43–50.

11. Brown S, Clastre M, Courdavault V, O'Connor SE: **De novo production of the plant-derived alkaloid strictosidine in yeast**. *Proc Natl Acad Sci U S A* 2015, **112**:3205–3210.

12. Kulagina N, Guirimand G, Melin C, Lemos-Cruz P, Carqueijeiro I, De Craene J-O, Oudin A, Heredia V, Koudounas K, Unlubayir M, et al.: **Enhanced bioproduction of anticancer precursor vindoline by yeast cell factories.** *Microb Biotechnol* 2021, **14**:2693–2699.

13. Liu T, Huang Y, Jiang L, Dong C, Gou Y, Lian J: **Efficient production of vindoline from tabersonine by metabolically engineered Saccharomyces cerevisiae**. *Commun Biol* 2021, **4**:1089.

14. Carqueijeiro I, Koudounas K, Dugé de Bernonville T, Sepúlveda LJ, Mosquera A, Bomzan DP, Oudin A, Lanoue A, Besseau S, Lemos Cruz P, et al.: **Alternative splicing creates a pseudo-strictosidine β-d-glucosidase modulating alkaloid synthesis in Catharanthus roseus**. *Plant Physiol* 2021, **185**:836–856.

15. Stavrinides A, Tatsis EC, Foureau E, Caputi L, Kellner F, Courdavault V, O'Connor SE: **Unlocking the Diversity of Alkaloids in Catharanthus roseus: Nuclear Localization Suggests Metabolic Channeling in Secondary Metabolism**. *Chem Biol* 2015, **22**:336–341.

16. Costa MMR, Hilliou F, Duarte P, Pereira LG, Almeida I, Leech M, Memelink J, Barceló AR, Sottomayor M: **Molecular cloning and characterization of a vacuolar class III peroxidase involved in the metabolism of anticancer alkaloids in Catharanthus roseus**. *Plant Physiol* 2008, **146**:403–417.

17. Stavrinides A, Tatsis EC, Caputi L, Foureau E, Stevenson CEM, Lawson DM, Courdavault V, O'Connor SE: **Structural investigation of heteroyohimbine alkaloid synthesis reveals active site elements that control stereoselectivity**. *Nat Commun* 2016, **7**:12116.

18••. Tatsis EC, Carqueijeiro I, Dugé de Bernonville T, Franke J, Dang T-TT, Oudin A, Lanoue A, Lafontaine F, Stavrinides AK, Clastre M, et al.: **A three enzyme system to generate the Strychnos alkaloid scaffold from a central biosynthetic intermediate**. *Nat Commun* 2017, **8**:316.

Identification and characterization of the two missing enzymes (GS and GO) downstream SGD, that convert strictosidine aglycone, or more specifically one of its more stable forms 4,21-dehydrogeissoschizine into akuammicine. While GO is an ER anchored cytochrome P450, GS displayed nucleo-cytosolic localization.

19. Qu Y, Thamm AMK, Czerwinski M, Masada S, Kim KH, Jones G, Liang P, De Luca V: **Geissoschizine synthase controls flux in the formation of monoterpenoid indole alkaloids in a Catharanthus roseus mutant.** *Planta* 2018, **247**:625–634.

20• . Qu Y, Easson MEAM, Simionescu R, Hajicek J, Thamm AMK, Salim V, De Luca V: **Solution of the multistep pathway for assembly of corynanthean, strychnos, iboga, and aspidosperma monoterpenoid indole alkaloids from 19E-geissoschizine**. *Proc Natl Acad Sci U S A* 2018, **115**:3180–3185.

Identification and characterization of the Redox 1, Redox 2 and SAT enzymes downstream GS and GO. Redox 1 and Redox 2 are thought to act in tandem to produce stemmadenine, which is further acetylated by SAT.

21•. Caputi L, Franke J, Farrow SC, Chung K, Payne RME, Nguyen TD, Dang TTT, Teto Carqueijeiro IS, Koudounas K, De Bernonville TD, et al.: **Missing enzymes in the biosynthesis of the anticancer drug vinblastine in Madagascar periwinkle**. *Science (80-)* 2018, **360**:1235–1239.

Identification and characterization of the two missing enzymes (PAS and DPAS) downstream SAT, which isomerize stemmadenine acetate into dihydroprecondylocarpine acetate. Subsequently, dihydroprecondylocarpine acetate is further converter into either tabersonine or catharanthine by TS or CS, respectively. While DPAS displayed interaction with TS and CS in the cytosol, PAS was shown to be targeted to the vacuole via putative ER vesicles.

22•. Qu Y, Safonova O, De Luca V: **Completion of the canonical pathway for assembly of anticancer drugs vincristine/vinblastine in Catharanthus roseus**. *Plant J* 2019, **97**:257–266.

The description of *O*-acetylstemmadenine oxidase (ASA or PAS) that converts *O*-acetylstemmadenine to reactive acetylated intermediates. In addition, two additional hydrolases were shown to convert PAS/DPAS product into vincadifformine, and GS is reported to manifest a second function - the reduction of ASO/PAS product.

23. Kellner F, Geu-Flores F, Sherden NH, Brown S, Foureau E, Courdavault V, O'Connor SE: **Discovery of a P450-catalyzed step in vindoline biosynthesis: a link between the aspidosperma and eburnamine alkaloids**. *Chem Commun* 2015, **51**:7626–7628.

24. Qu Y, Easson MLAE, Froese J, Simionescu R, Hudlicky T, DeLuca V: **Completion of the seven-step pathway from tabersonine to the anticancer drug precursor vindoline and its assembly in yeast**. *Proc Natl Acad Sci U S A* 2015, **112**:6224–6229.

25. Deluca V, Balsevich J, Tyler RT, Kurz WG: **Characterization of a novel N-methyltransferase (NMT) from Catharanthus roseus plants : Detection of NMT and other enzymes of the indole alkaloid biosynthetic pathway in different cell suspension culture systems.** *Plant Cell Rep* 1987, **6**:458–461.

26. Koudounas K, Guirimand G, Hoyos LFR, Carqueijeiro I, Cruz PL, Stander E, Kulagina N, Perrin J, Oudin A, Besseau S, et al.: **Tonoplast and Peroxisome Targeting of γ-tocopherol N-methyltransferase Homologs Involved in the Synthesis of Monoterpene Indole Alkaloids**. *Plant Cell Physiol* 2021, doi:10.1093/pcp/pcab160.

27. St-Pierre B, Vazquez-Flota FA, V DL: **Multicellular compartmentation of catharanthus roseus alkaloid biosynthesis predicts intercellular translocation of a pathway intermediate**. *Plant Cell* 1999, **11**:887–900.

28. Carqueijeiro I, Brown S, Chung K, Dang T-T, Walia M, Besseau S, Dugé de Bernonville T, Oudin A, Lanoue A, Billet K, et al.: **Two Tabersonine 6,7-Epoxidases Initiate Lochnericine-Derived Alkaloid Biosynthesis in Catharanthus roseus**. *Plant Physiol* 2018, **177**:1473–1486.

29. Giddings LA, Liscombe DK, Hamilton JP, Childs KL, DellaPenna D, Buell CR, O'Connor SE: **A stereoselective hydroxylation step of alkaloid biosynthesis by a unique cytochrome P450 in Catharanthus roseus**. *J Biol Chem* 2011, **286**:16751–16757.

30. Carqueijeiro I, Dugé de Bernonville T, Lanoue A, Dang T-T, Teijaro CN, Paetz C, Billet K, Mosquera A, Oudin A,

Besseau S, et al.: **A BAHD acyltransferase catalyzing 19-O-acetylation of tabersonine derivatives in roots of Catharanthus roseus enables combinatorial synthesis of monoterpene indole alkaloids**. *Plant J* 2018, **94**:469–484.

31. Williams D, Qu Y, Simionescu R, De Luca V: **The assembly of (+)-vincadifformine- and (−)-tabersonine-derived monoterpenoid indole alkaloids in Catharanthus roseus involves separate branch pathways**. *Plant J* 2019, **99**:626–636.

32. Laflamme P, St.-Pierre B, De Luca V: **Molecular and biochemical analysis of a Madagascar periwinkle root-specific minovincinine-19-hydroxy-o-acetyltransferase**. *Plant Physiol* 2001, **125**:189–198.

33. Miettinen K, Dong L, Navrot N, Schneider T, Burlat V, Pollier J, Woittiez L, Van Der Krol S, Lugan R, Ilc T, et al.: **The seco-iridoid pathway from Catharanthus roseus**. *Nat Commun* 2014, **5**.

34•. Larsen B, Fuller VL, Pollier J, Van Moerkercke A, Schweizer F, Payne R, Colinas M, O'Connor SE, Goossens A, Halkier BA: **Identification of Iridoid Glucoside Transporters in Catharanthus roseus**. *Plant Cell Physiol* 2017, **58**:1507–1518.

Identification of MIA transporters from the nitrate/peptide family (NPF), which were shown to import loganic acid, loganin and secologanin in *Xenopus laevis* oocytes.

35. Kidd T, Easson MLAE, Qu Y, De Luca V: **Inter-organ transport of secologanin allows assembly of monoterpenoid indole alkaloids in a Catharanthus roseus mutant**. *Phytochemistry* 2019, **159**:119–126.

36. Guirimand G, Guihur A, Perello C, Phillips M, Mahroug S, Oudin A, Dugé de Bernonville T, Besseau S, Lanoue A, Giglioli-Guivarc'h N, et al.: **Cellular and Subcellular Compartmentation of the 2C-Methyl-D-Erythritol 4-Phosphate Pathway in the Madagascar Periwinkle.** *Plants (Basel, Switzerland)* 2020, **9**.

37••. Payne RME, Xu D, Foureau E, Teto Carqueijeiro MIS, Oudin A, Bernonville TD de, Novak V, Burow M, Olsen C-E, Jones DM, et al.: **An NPF transporter exports a central monoterpene indole alkaloid intermediate from the vacuole.** *Nat plants* 2017, **3**:16208.

Identification of tonoplast-localized NPF transporter that exports strictosidine from the vacuole into the cytosol.

38. Carqueijeiro I, Noronha H, Duarte P, Gerós H, Sottomayor M: **Vacuolar transport of the medicinal alkaloids from Catharanthus roseus is mediated by a proton-driven antiport.** *Plant Physiol* 2013, **162**:1486–1496.

39. Yu F, De Luca V: **ATP-binding cassette transporter controls leaf surface secretion of anticancer drug components in Catharanthus roseus.** *Proc Natl Acad Sci U S A* 2013, **110**:15830–15835.

40. Dugé de Bernonville T, Carqueijeiro I, Lanoue A, Lafontaine F, Sánchez Bel P, Liesecke F, Musset K, Oudin A, Glévarec G, Pichon O, et al.: **Folivory elicits a strong defense reaction in Catharanthus roseus: metabolomic and transcriptomic analyses reveal distinct local and systemic responses**. *Sci Rep* 2017, **7**:40453.

41. Roepke J, Salim V, Wu M, Thamm AMK, Murata J, Ploss K, Boland W, De Luca V: **Vinca drug components accumulate exclusively in leaf exudates of Madagascar periwinkle**. *Proc Natl Acad Sci* 2010, **107**:15287 LP – 15292.

42. Abouzeid S, Hijazin T, Lewerenz L, Hänsch R, Selmar D. **The genuine localization of indole alkaloids in Vinca minor and Catharanthus roseus**. *Phytochemistry*. 2019 Dec;168:112110.

43. Yamamoto K, Takahashi K, Mizuno H, Anegawa A, Ishizaki K, Fukaki H, Ohnishi M, Yamazaki M, Masujima T, Mimura T: **Cell-specific localization of alkaloids in Catharanthus roseus stem tissue measured with Imaging MS and Single-cell MS.** *Proc Natl Acad Sci U S A* 2016, **113**:3891–6.

44••. Yamamoto K, Takahashi K, Caputi L, Mizuno H, Rodriguez-Lopez CE, Iwasaki T, Ishizaki K, Fukaki H, Ohnishi M, Yamazaki M, et al.: **The complexity of intercellular localisation of alkaloids revealed by single-cell metabolomics**. *New Phytol* 2019, **224**:848–859.

MALDI imaging confirmed most MIA (putative) localization, except catharanthine, which likewise vindoline was detected in idioblasts/laticifers.

45. Nakabayashi R, Mori T, Takeda N, Toyooka K, Sudo H, Tsugawa H, Saito K: **Metabolomics with 15N Labeling for Characterizing Missing Monoterpene Indole Alkaloids in Plants**. *Anal Chem* 2020, **92**:5670–5675.

46•. Nakabayashi R, Takeda-Kamiya N, Yamada Y, Mori T, Uzaki M, Nirasawa T, Toyooka K, Saito K: **A multimodal metabolomics approach using imaging mass spectrometry and liquid chromatography-tandem mass spectrometry for spatially characterizing monoterpene indole alkaloids secreted from roots.** *Plant Biotechnol (Tokyo, Japan)* 2021, **38**:305–310.

Catharanthine, ajmalicine, serpentine and yohimbine were identified in *C. roseus* root environment using IMS and LC-MS/MS indicating root secretion.

47. Dugé de Bernonville T, Maury S, Delaunay A, Daviaud C, Chaparro C, Tost J, O'Connor SE, Courdavault V: **Developmental Methylome of the Medicinal Plant Catharanthus roseus Unravels the Tissue-Specific Control of the Monoterpene Indole Alkaloid Pathway by DNA Methylation**. *Int J Mol Sci* 2020, **21**.

48. Marand AP, Schmitz RJ: **Single-cell analysis of cis-regulatory elements**. *Curr Opin Plant Biol* 2022, **65**:102094.

49. Li X, Cai W, Liu Y, Li H, Fu L, Liu Z, Xu L, Liu H, Xu T, Xiong Y: **Differential TOR activation and cell proliferation in Arabidopsis root and shoot apexes.** *Proc Natl Acad Sci U S A* 2017, **114**:2765–2770.

50. VanInsberghe M, van den Berg J, Andersson-Rolf A, Clevers H, van Oudenaarden A: **Single-cell Ribo-seq reveals cell cycle-dependent translational pausing**. *Nature* 2021, **597**:561–565.

51. Dai X, Tu X, Du B, Dong P, Sun S, Wang X, Sun J, Li G, Lu T, Zhong S, et al.: **Chromatin and regulatory differentiation between bundle sheath and mesophyll cells in maize.** *Plant J* 2021, doi:10.1111/tpj.15586.

52. Rai A, Hirakawa H, Nakabayashi R, Kikuchi S, Hayashi K, Rai M, Tsugawa H, Nakaya T, Mori T, Nagasaki H, et al.: **Chromosome-level genome assembly of Ophiorrhiza pumila reveals the evolution of camptothecin biosynthesis**. *Nat Commun* 2021, **12**:405.

53. Bharadwaj R, Kumar SR, Sharma A, Sathishkumar R: **Plant Metabolic Gene Clusters: Evolution, Organization, and Their Applications in Synthetic Biology** . *Front Plant Sci* 2021, **12**:1573.

54. Liu GS, Li T, Zhou W, Jiang M, Tao XY, Liu M, Zhao M, Ren YH, Gao B, Wang FQ, et al.: **The yeast peroxisome: A dynamic storage depot and subcellular factory for squalene overproduction**. *Metab Eng* 2020, **57**:151–161.

55. Dusséaux S, Wajn WT, Liu Y, Ignea C, Kampranis SC: **Transforming yeast peroxisomes into microfactories for the efficient production of high-value isoprenoids**. *Proc Natl Acad Sci U S A* 2020, **117**:31789–31799.

56. Grewal PS, Samson JA, Baker JJ, Choi B, Dueber JE: **Peroxisome compartmentalization of a toxic enzyme improves alkaloid production**. *Nat Chem Biol* 2021, **17**:96–103.

57. Gerke J, Frauendorf H, Schneider D, Wintergoller M, Hofmeister T, Poehlein A, Zebec Z, Takano E, Scrutton NS, Braus GH: **Production of the Fragrance Geraniol in Peroxisomes of a Product-Tolerant Baker's Yeast**. *Front Bioeng Biotechnol* 2020, **8**.

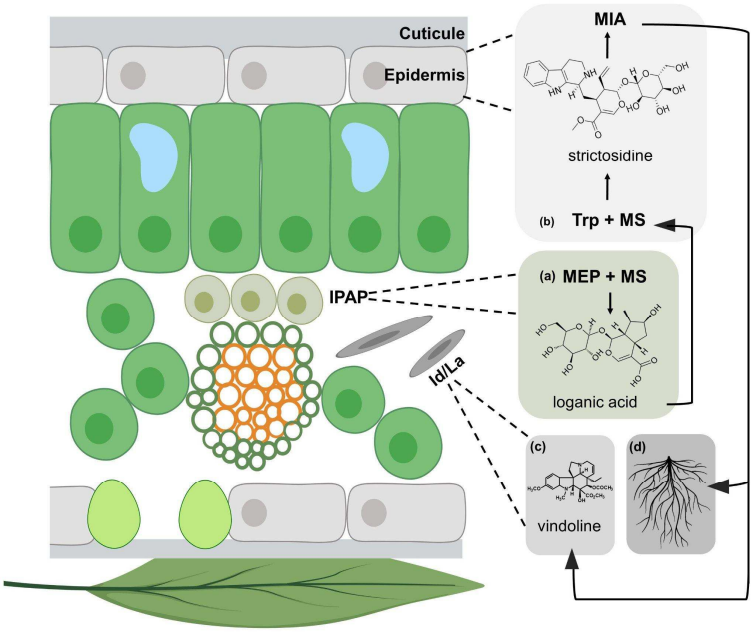

Figure 1. A simplified overview of *C. roseus* MIA metabolism. IPAP: internal phloem associated parenchyma cells; Id: idioblasts; La: laticifers; MEP: methylerythritol 4-phosphate pathway; MS: monoterpene secoiridoid pathway; MIA: monoterpene indole alkaloid pathway. The MIA pathway architecture integrates several tissues and organs, which also involves subcellular organization and intermediate translocation detailed in Figure 2. The loganic acid is synthesized in IPAP cells via MEP and MS pathways (a), followed by the formation of strictosidine in epidermal cells (b) - the central MIA precursor, and downstream MIAs. Vindoline, the aspidosperma type MIA is further produced in Id and La cells (c) while root-specific heteroyohimbine-type MIAs are synthesized in roots (d). The figure was created with BioRender.com.

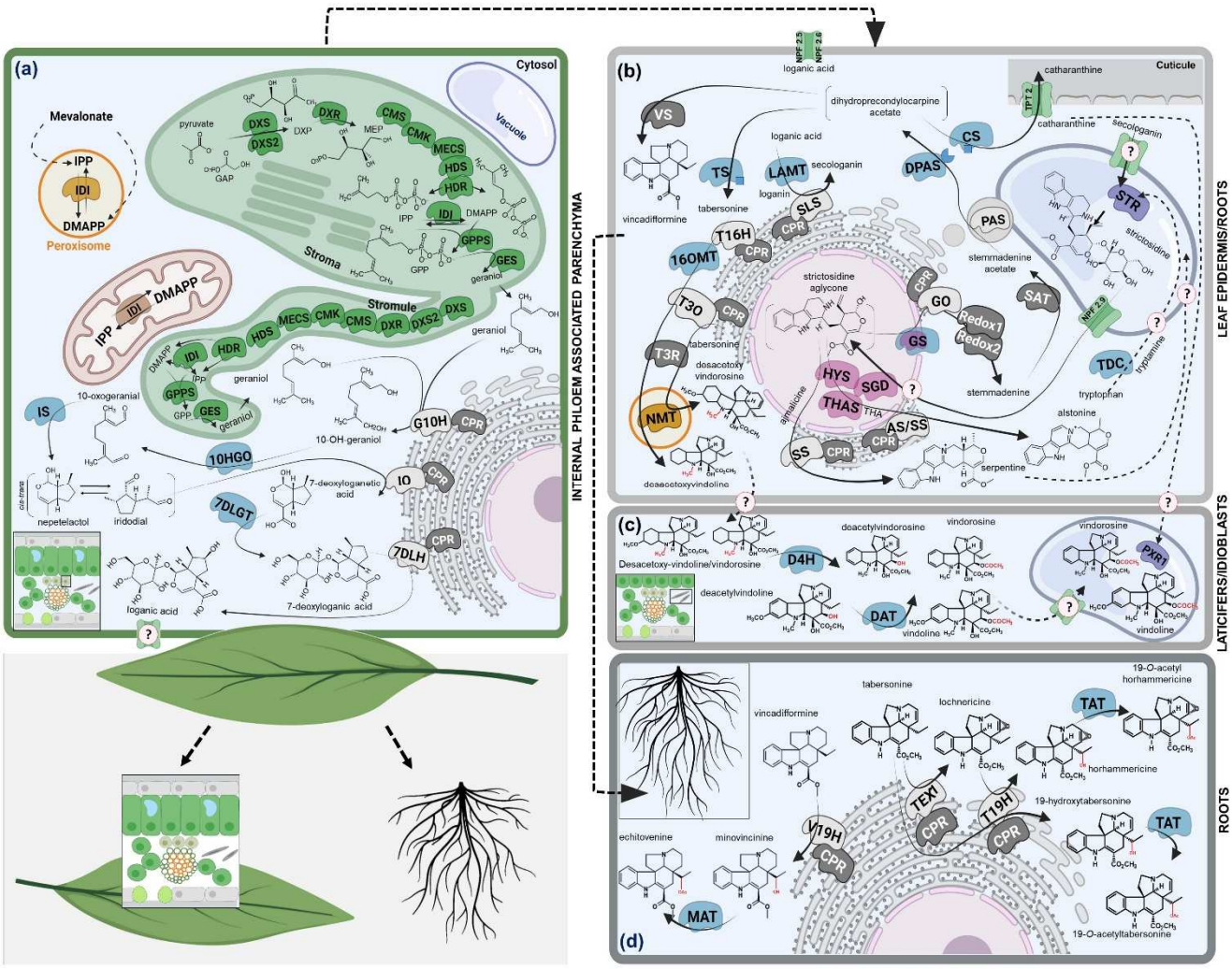

Figure 2. ***C. roseus*** **MIA pathway architecture (adapted and updated from [10]).** MIA biosynthesis implicates several tissue/cell types and organs starting with internal phloem associated parenchyma (IPAP) that hosts both the methyl-erythritol phosphate pathway and the beginning of the monoterpene-iridoid pathway (**a**), followed by the downstream enzymatic steps in the epidermis (**b**), laticifers and idioblasts (**c**), and roots (**d**). DXS, 1-deoxy-D-xylulose-5-phosphate (DXP) synthase; DXR, DXP reductoisomerase, CMS, 4-(cytidine 5'-diphospho)-2C-methyl-D-erythritol (CM) synthase; CMK, CM kinase; MECS, 2C-methyl-D-erythritol-2,4-cyclodiphosphate (MEC) synthase; HDS, hydroxymethylbutenyl 4-diphosphate (HD) synthase; HDR, HD reductase; IDI, isopentenyl diphosphate isomerase; GPPS, geranyl diphosphate synthase; GES, geraniol synthase; G10H, geraniol 10-hydroxylase; CPR, cytochrome P450-reductase; 10HGO, 10-hydroxygeraniol oxidoreductase; IS, iridoid synthase; IO, iridoid oxidase; 7DLGT, 7-deoxyloganetic acid glucosyltransferase; 7DLH, 7-deoxyloganic acid hydroxylase; IPP, isopentenyl pyrophosphate; DMAPP, dimethylallyl pyrophosphate; LAMT, loganic acid *O*-methyltransferase; SLS, secologanin synthase; TDC, tryptophan decarboxylase; STR, strictosidine synthase; SGD, strictosidine β-glucosidase; HYS, heteroyohimbine synthase (interacts with SGD and self-interacts); THAS, tetrahydroalstonine (THA) synthase (interacts with SGD and self-interacts); AS, alstonine synthase; SS, seprentine synthase; GS, geissoschizine synthase; GO, geissoschizine oxidase; Redox 1, cinnamyl alcohol dehydrogenase-like; Redox 2, aldo-keto-type reductase; SAT, stemmadenine-*O*-acetyltransferase; PAS, precondylocarpine acetate synthase, DPAS, dihydroprecondylocarpine synthase (interacts with CS and preferentially with TS, the interactions are indicated with small blue sector and squares); CS, catharanthine synthase; TS, tabersonine synthase; VS, vincadifformine synthase; T16H, tabersonine 16-hydroxylase; 16OMT, 16-hydroxytabersonine *O*-methyltransferase; T3O, tabersonine 3-oxygenase (can directly epoxidize tabersonine, which results in a side metabolic branch and downstream conversion to vindorosine); T3R, tabersonine 3-reductase; NMT, 16-methoxy-2,3-dihydro-3-hydroxytabersonine *N*-methyltransferase (the tissular localization is unclear); TPT2, catharanthine ABC transporter; D4H, desacetoxyvindoline 4-hydrolase; DAT, deacetylvindoline 4-O-acetyltransferase; NPF, nitrate/peptide family of transporters; PXR1, vacuolar class III peroxidase; TEX 1, tabersonine 6,7-epoxidase isoform 1; T19H, tabersonine 19-hydrolase (can hydroxylate both, tabersonine and lochnericine); V19H, vincadifformine 19-hydrolase; MAT, minovincine 19-hydroxy-*O*-acetyltransferase; TAT, tabersonine 19-*O*-acetyltransferase. Enzyme localization is color-coded: green - chloroplast stroma/stromules; brown - mitochondria; orange - peroxisome; blue - cytoplasm; gray - ER; dark gray - subcellular localization that was not confirmed by microscopy imaging; purple - vacuole; pink - nucleus; GS dual pink-blue color illustrates nucleo-cytoplasmic localization. Plain arrows indicate enzymatic steps, thin dashed arrows represent uncharacterized transport of metabolites, intra- or intercellular. When applicable, tissue/cell types are displayed in the left corner of subfigures. The figure was created with BioRender.com.

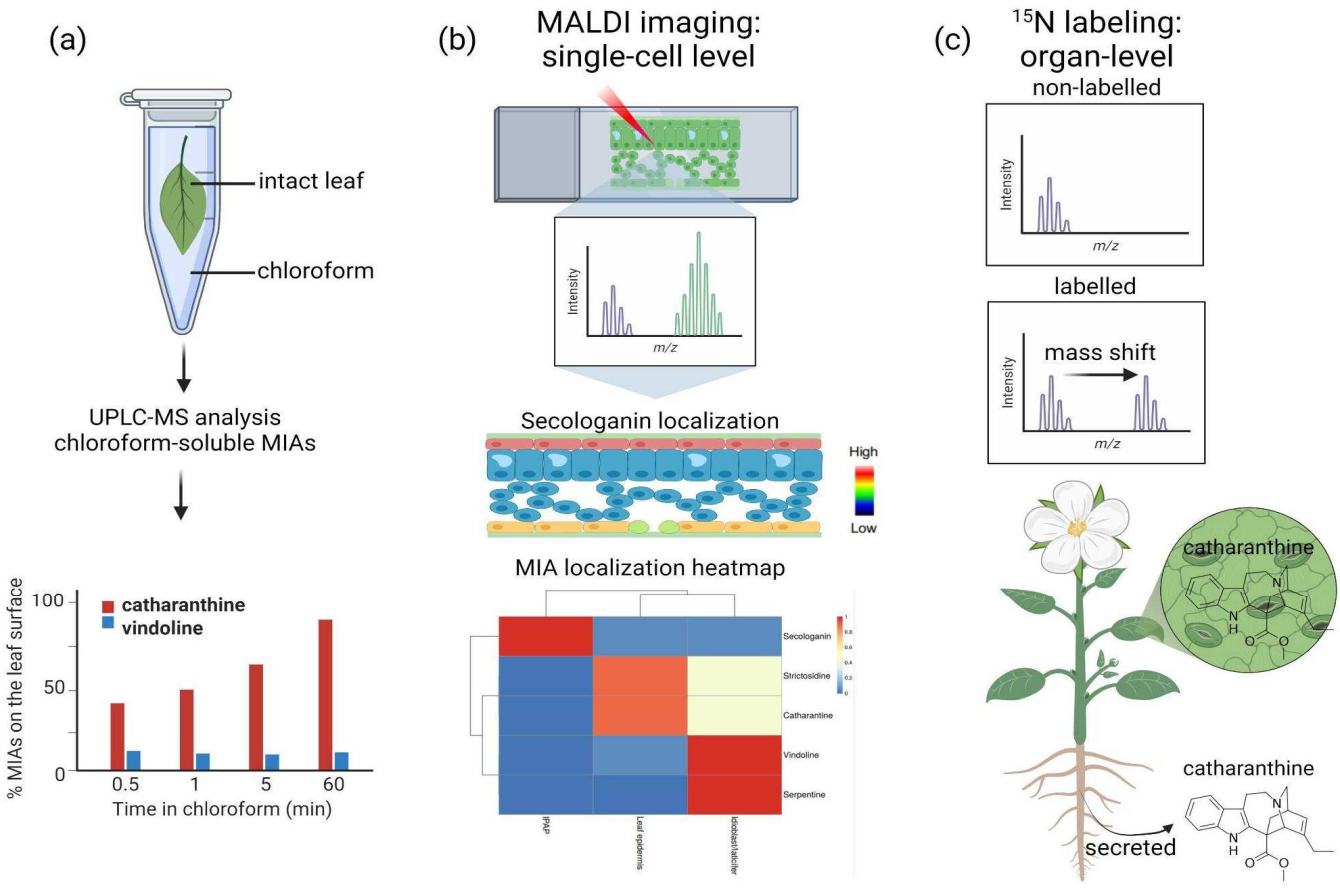

Figure 3. MALDI imaging and metabolic labeling revealed MIA localization. (**a**) Whole *C. roseus* intact leaves were dipped in chloroform to extract leaf surface MIAs. On the contrary to vindoline, catharanthine was efficiently solubilized by chloroform dipping [41]**.** (**b**) MALDI imaging of matrix-embedded tissues has allowed single-cell localization and quantification of certain MIAs in the stem [43] and leaves [44••] of *C. roseus* at 10 µm resolution. A schematic representation of secologanin quantitative localization is shown. The heatmap was constructed using relative quantification data from [44••]. (**c**) Metabolic labeling of *C. roseus* plants via N radiolabeling, and comparison with non-labeled samples has allowed the detection of catharanthine, and previously undetected MIAs, in the root external environment in addition to leaves [45,46•]. The figure was created with BioRender.com.